Hindawi
Advances in Materials Science and Engineering
Volume 2022, Article ID 7488254, 16 pages
https://doi.org/10.1155/2022/7488254

*Research Article*

# Experimental Analysis of Geopolymer Concrete: A Sustainable and Economic Concrete Using the Cost Estimation Model

**Manvendra Verma**[1], **Kamal Upreti**[2], **Prashant Vats**[3], **Sandeep Singh**[3], **Prashant Singh**[4], **Nirendra Dev**[1], **Durgesh Kumar Mishra**[5] and **Basant Tiwari**[6]

[1]*Department of Civil Engineering, Delhi Technological University, Delhi, India*
[2]*Department of Computer Science & Engineering, Dr. Akhilesh Das Gupta Institute of Engineering & Technology, New Delhi, India*
[3]*Department of Computer Science and Engineering, Faculty of Engineering and Technology, SGT University, Gurugram, Haryana, India*
[4]*Department of Computer Science & Engineering, JSS Academy of Technical Education, Noida, India*
[5]*Department of Computer Science & Engineering, Sri Aurobindo Institute of Technology, Indore, India*
[6]*Deparent of Computer Science IoT, Hawassa University, Hawassa, Ethiopia*

Correspondence should be addressed to Basant Tiwari; basanttiw@hu.edu.et

Received 30 July 2022; Revised 14 August 2022; Accepted 17 August 2022; Published 6 October 2022

Academic Editor: Samson Jerold Samuel Chelladurai



Geopolymer concrete is sustainable, economical, eco-friendly, durable, and high-strength concrete. Geopolymer is a name for the bonding that occurs during the binding of materials in alkaline conditions. Due to the presence of high silica and alumina content, pozzolanic materials could be used as binding materials in the GPC. This research aims to check the sustainability and cost analysis of both GPC and conventional concrete with their physical, chemical, and mechanical properties. The experimental investigation analyzes both GPC and OPC concrete's physical, chemical, and mechanical properties for the M30 mix design and analyzes the concrete's cost and sustainability. The experimental investigation shows that the setting time, density, and drying shrinkage of conventional concrete are higher than the GPC. The compressive strength of the GPC and OPC concretes both showed similar trends at the 28-day strength, but the initial three-day strength of the GPC concrete was much higher than the OPC concrete. The splitting tensile strength and flexural strength of the GPC specimens are slightly higher than the OPC concrete mix specimens. The OPC concrete's elastic modulus is slightly higher than the GPC mix design, whereas the Poisson's ratio of the OPC concrete is slightly lower than the GPC specimens. The GPC specimens have higher thermal stability up to 800°C. The GPC utilizes industrial solid waste like fly ash and slag as a binding material and is activated by an alkaline solution containing NaOH and $Na_2SiO_3$ in the design mix. Therefore, the GPC has less embodied energy compared to the OPC concrete. The cost of the GPC at a bulk level reduced the cost of up to 40% of the OPC concrete.

## 1. Introduction

GPC has become a perfect alternative to the world's sustainable construction industry because the concrete demand is the second largest in the world after water. The expansion of infrastructure accelerates the development of the country and society. So, concrete production will increase exponentially in the future with development. A comparable amount of carbon is emitted into the environment during the production of OPC cement. In the GPC, industrial solid waste, fly ash, and slag are used. Fly ash is generated in thermal power plants as a waste product in vast amounts, but the utilization of fly ash is limited to up to 50% of the production [1]. GPC shows better physical, chemical, and mechanical properties compared to OPC cement concrete. The durability properties of the GPC are also higher than those of OPC concrete. GPC concrete is more sulfate-resistant than OPC concrete [2–5]. The geopolymerisation

reaction plays a vital role in developing the strength of the GPC, and some factors affect the geopolymerisation process, like curing conditions, alkaline solution content, and binding material content in the design mix.

Due to the high silica and alumina content composition, pozzolanic materials like fly ash, GGBFS, metakaolin, and rice husk ash were used as binding materials in the geopolymer. The compressive strength increases with the Si/Al ratio [6]. The sodium hydroxide and sodium silicate mix solutions were used to activate the pozzolanic material to work as a binding material for the geopolymerisation reaction. The GPC mix's strength increases with NaOH's molarity increment, reducing workability [7–12]. The geopolymerisation reaction develops the concrete's strength, which is affected by various factors and parameters. The alkaline ratio also affects the mix's strength, increasing with the $Na_2SiO_3$/NaOH ratio [13].

The curing condition is an essential parameter for gaining strength, and the strength increases with the increment of the curing temperature up to 100°C [14, 15]. The replacement of fly ash by the GGBFS develops the GPC mix's strength in ambient curing conditions [16]. The fineness of the flux plays a vital role in the development of strength; it increases strength and decreases the mix's setting time [17, 18]. The fineness of fly ash reduces porosity directly by increasing the number of small particles in the mix [19, 20]. In the geopolymerisation reaction, curing time affects the mix's early strength development, and a longer curing time gives better end products after the reaction [21]. The water present in the mix was not used in the geopolymerisation end products, so water evaporation made the specimens crack-free [22, 23]. As a result, the water content of the mix increases, reducing the strength of the mixed specimens, and slag has a high potential for reactivity and bond formation for strength development [9, 24]. The GPC has a very high potential to resist the acidic or sea-water environment and other extreme weather conditions [25], and it shows the future scope of the geopolymer paste as a repair of the concrete structure due to its efficiency and performance [26]. GPC specimens are more resistant to high temperatures than OPC concrete samples [27]. Manufacturing sand or stone dust has a high capacity for fine aggregate in concrete without lowering its strength. It also contributes to the formation of high-strength GPC [28, 29]. All alternative materials used in building construction components have a lower energy level than conventional building materials [28–46].

Embodied energy is used to calculate the carbon footprints of various material production methods [47]. The GGBFS and fly ash content in the concrete's mix design reduce the concrete's embodied energy [48, 49]. The optimum point for mechanical properties is a GGBFS/Flash ratio of 20/80 [46]. The SNF-based superplasticizer is efficient for the mechanical properties of GPC [37], and the liquid-to-binder ratio plays a vital role in strength development [34]. The PCE-based superplasticizer is used to self-compact conventional concrete [31]. The study successfully reused waste rubber tyres and waste wood ash by developing sustainable geopolymer concrete that could be utilized for construction industry applications to create various construction and concrete products [50]. GPC is more resistant to various durability conditions than OPC concrete [33, 51, 52].

## 2. Experimental Program

*2.1. Binding Materials.* All the constituents used in forming the GPC and OPC concrete specimens for the experimental analysis are explained separately in the paragraphs. The preliminary test on the material samples was to identify the concrete laboratory properties in the civil engineering department, DTU, Delhi. The SEM and EDS tests of the samples were done in the nanotechnology lab, Jamia Millia Islamia, New Delhi, whereas the XRD test was done in the central facility laboratory, DTU, Delhi. The OPC 43 grade of cement was purchased from JK Cement to experiment with a controlled mix design [53]. In the preliminary check, the cement's quality is determined by testing consistency, initial and final setting time, specific gravity, fineness of the particle size, and soundness. The cement passes all preliminary tests as per Indian standard codes [56–62]. The cement's properties are identified through the testing of samples in the concrete laboratory in the civil engineering department, DTU, Delhi. Fly ash is an industrial solid waste produced by a thermal power plant from coal ash fumes and electrostatic precipitation. The particle size of the fly ash is slightly smaller or similar to that of the OPC particle size, and the composition contains a high concentration of silica and alumina. Fly ash was brought from the national thermal power plant, Dadri, Gautam Budh Nagar, Uttar Pradesh, India.

GGBFS is produced in the steel manufacturing plant by quenching the slag from the molten iron steel material. After separating the waste from steel manufacturing, the waste material present in the iron or steel ores is slag. GGBFS also contains a high silica and alumina content in the composition. GGBFS was brought from the Bhilai steel plant in Bhilai, Chhattisgarh, India, to test and produce the GPC mix specimens. Figure 1(a) shows the XRD graph of the GGBFS, which shows the sample's amorphous nature, whereas Table 1 shows the chemical composition present in the GGBFS sample. In addition, Figure 1(b) describes the SEM image of the GGBFS sample at a resolution of two microns and shows the irregular shape of the particles, whereas Figure 1(e) shows the EDS graph, which describes the elements present in the samples.

The fly ash used in the test is a mix-design class-c fly ash [54]. The particles of the fly ash are spherical and porous, as confirmed by the SEM image. Figure 1(a) shows the amorphous nature of the fly ash sample in the XRD graph, whereas Figure 1(c) shows the porous spherical particles of the fly ash in the SEM image at a 5-micron resolution. Table 1 shows the composition of the chemical constituents present in the fly ash as explained by the XRF test, and Figure 1(d) shows the EDS graph, which describes the element content present in the fly ash as conducted in the nanotechnology lab at Jamia Millia Islamia, New Delhi, India.

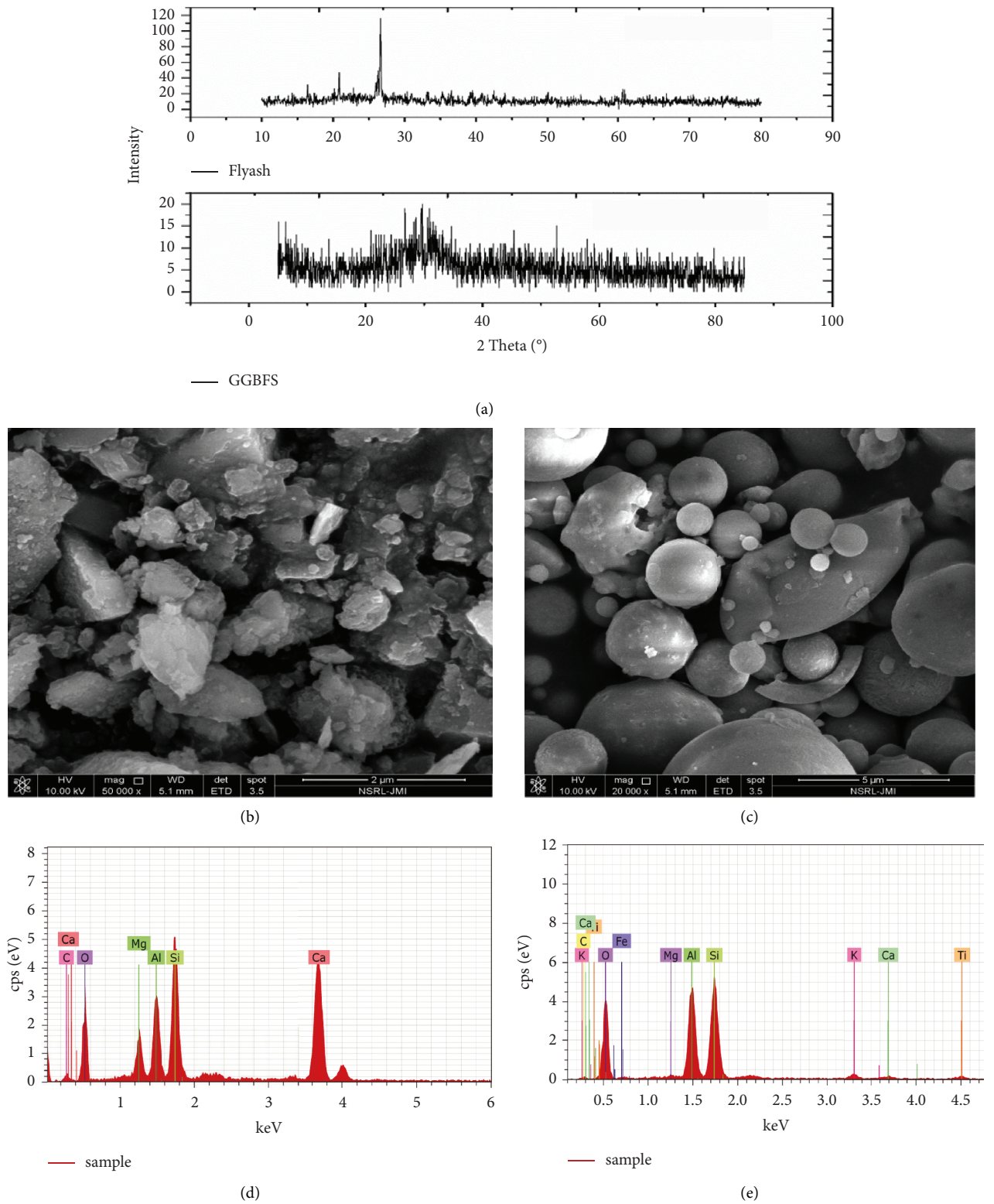


Figure 1: (a) XRD pattern of fly ash and GGBFS; (b) SEM image of GGBFS; (c) SEM image of fly ash; (d) EDS graph of fly ash; and (e) EDS graph of GGBFS.

*2.2. Alkaline Solution.* The alkaline solution plays a vital role in the geopolymerisation reaction because it activates the reaction's pozzolanic binding materials and finds the end products. For sampling, the alkaline solution contains sodium hydroxide and sodium silicate solution, and it is mixed for 20–24 hours. Sodium hydroxide was purchased from Fisher Scientific in the business park, Powai, Mumbai, Maharashtra, India. Figure 2(a) shows the sample of sodium

Table 1: Composition of fly ash and GGBFS.

| Characteristics | $SiO_2$ | $Al_2O_3$ | CaO | $Fe_2O_3$ | MgO | $SO_3$ | LOI |
|---|---|---|---|---|---|---|---|
| Flyash (%) | 45.8 | 21.4 | 13.7 | 12.6 | 1.3 | 1.9 | .1 |
| GGBFS (%) | 34.52 | 20.66 | 32.43 | .57 | 10.09 | .77 | .3 |

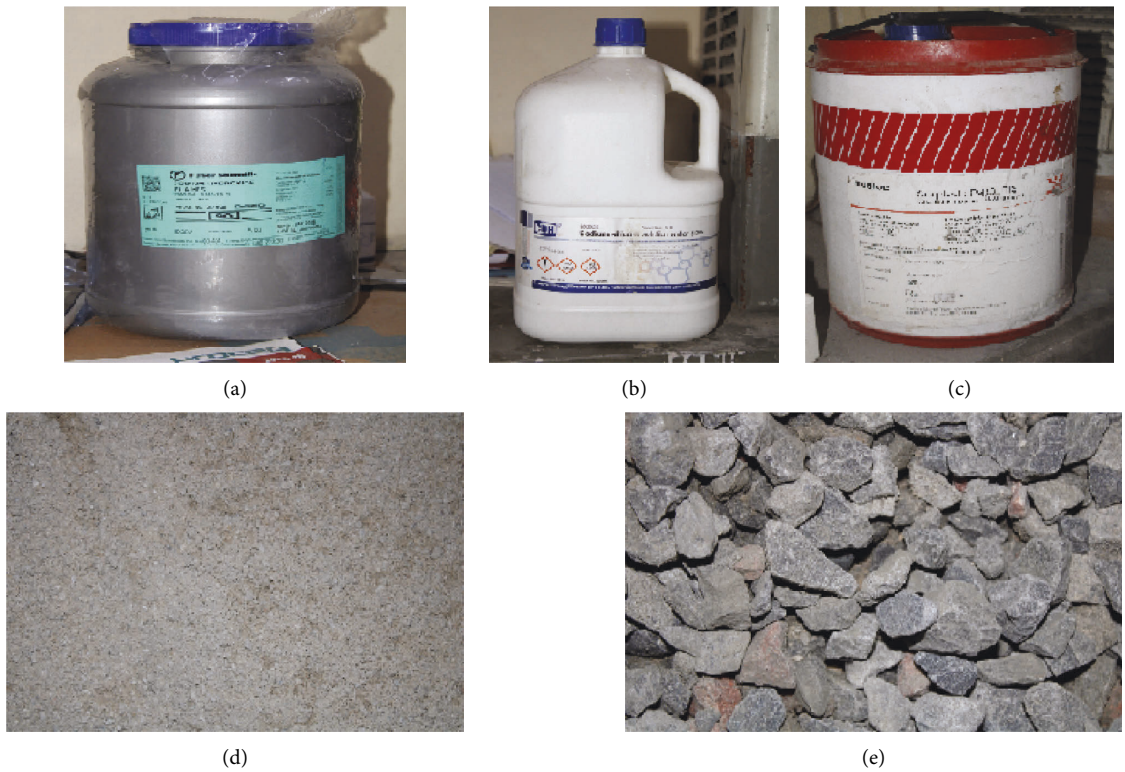


Figure 2: Picture of raw materials of the GPC (a) sodium hydroxide flakes, (b) sodium silicate solutions, (c) superplasticizer, (d) stone-dusts, and (e) coarse aggregates.

hydroxide flakes used in the mix design, whereas Figure 2(b) shows the sodium silicate sample purchased from the Central Drug House (P) Ltd.

*2.3. Aggregates.* Aggregate is used as the concrete's skeleton because it occupies up to 85% of the concrete. The aggregate used in the mix is primarily classified into two categories: fine aggregates and coarse aggregates. In the coarse aggregate, the two types of aggregates used are 10 mm and 20 mm in the design mix, whereas the fine aggregate is used as crushed stone dust in the mix of both concrete. To test the aggregate use quality in the mix design using Indian standard codes. In the preliminary test, check the gradation of the aggregates, zone, fineness modulus, specific gravity, water absorption, silt content, bulk density, crushing value, impact value, abrasion value, flakiness index, and elongation index of the aggregate samples [55–60]. Figure 2(d) depicts the raw material of stone dust used as a fine aggregate in the mixed design. Figure 3 describes the grain-size curve on the logarithmic graph and the particle size distribution or gradation of the m-sand by the sieve analysis. The stone-dust properties were found through the tests conducted in the concrete lab.

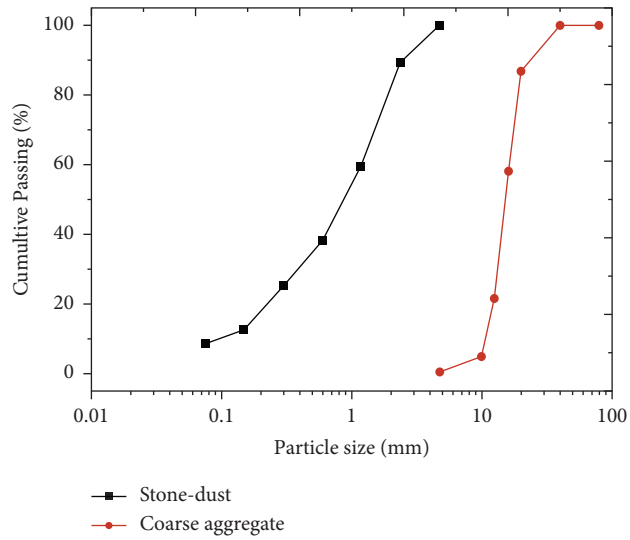


Figure 3: Grain size distribution curve.

As the percentage passing the 600$\mu$ sieve is between 35 and 59, the sand belongs to gradation II. From the gradation curve, we find $D_{10} = 0.1$, $D_{30} = 0.4$, and $D_{60} = 1.2$.

Table 2: Mix proportion of GPC and OPC concrete.

| Constituents | OPC concrete mix content (kg/m$^3$) | Geopolymer concrete mix content (kg/m$^3$) |
|---|---|---|
| OPC | 370 | 00 |
| Flyash | 00 | 303.75 |
| GGBFS | 00 | 101.25 |
| NaOH | 00 | 40.5 |
| $Na_2SiO_3$ | 00 | 101.25 |
| Fine aggregate | 683 | 683 |
| Coarse aggregate | 1289 | 1269 |
| Water | 148 | 40.5 |
| Superplasticiser | 3.7 | 4.05 |
| Total | 2493.7 | 2543.7 |

$$\text{Cu} = D_{60}/D_{10} = 1.2/0.1 = 12 > 6.$$

$$C_c = (D_{30})^2/(D_{10} \text{ x } D_{60}) = 0.4^2/(0.1 \times 1.2) = 1.33.$$

Thus, the sand is well-graded.

Locally available materials, coarse aggregates, are used in all mixes of concrete. The particle size of aggregates present in the sample was determined by their percentage and found the coarse aggregate's fineness modulus. The coarse aggregate properties were discovered through laboratory tests under Indian standards. Figure 2(e) depicts coarse aggregate sample images, whereas coarse aggregate properties are discovered through laboratory tests following Indian standards. The fineness modulus of the coarse aggregate is 7.29, calculated through the sieve analysis of the samples.

*2.4. Superplasticiser.* The superplasticiser enhances the concrete's performance by reducing the mix design's water content and increasing the fresh mix's workability [61]. The SNF-based superplasticizer is used in the mix design of both concrete made by the Fosroc industry named SP Conplast-430 in the market. Figure 2(c) shows that the picture of the superplasticizer used in the experimental investigation.

*2.5. Sampling and Test Setups.* Specimens made of the controlled OPC concrete mix usually mix all constituents into the pan mixture for around 2 to 5 minutes and are cast in the specimen mould for 24 hours. In GPC, the alkaline solution mixes before 20–24 hours of mixing the concrete constituents in the pan mixture and is cast in the mould of the specimens with the proper compaction of the casted samples [62–65]. The OPC concrete specimens were cured in the water tank, but the GPC specimens were cured in the oven at 60°C for 24 hours. The cubical, cylindrical, and beam-shaped specimens were cast out of both types of concrete for testing. Physical and mechanical properties were tested for both types of concrete. Table 2 describes the mixed proportion of all constituents used in GPC and OPC concrete's mixed design.

*2.6. Physical Properties.* The slump and compaction factor tests are used for the identification of the workability of the concrete. Slump is most commonly used for testing the workability of concrete on-site or in the laboratory, whereas the compaction factor is only used in the laboratory. The slump is conical in shape, but the compaction factor setup comprises two conical-shaped buckets fitted in vertical alignment with a standard gap, allowing the buckets' surface to be opened. The compaction factor checks the self-compaction ability of the concrete with gravity force [64, 66]. Self-compacting concrete is made using a PCE-based superplasticizer in the concrete mix design.

*2.6.1. Chemical Properties.* The weight of the specimens was calculated from the density of both mixed specimens before the destructive tests. Thus, the cube specimen's weight determines the mixed density 28 days after the casting, and the mass calculates the density-to-volume ratio of the cube specimens [67].

*2.6.2. Mechanical Properties Tests.* The compressive strength of both types of concrete mixes was tested by the cube sample test under the CTM machine at the 5.25 kN/sec rate of the loading statically applied to the specimens. The cube sizes of 150 mm × 150 mm $x$ 150 mm follow the Indian standard code. The mixed samples were tested 3, 7, 14, and 28 days after the specimens were cast [68, 69].

Splitting tensile is used to find the indirect tensile strength of the concrete. According to the Indian standard codes used to determine the splitting tensile of concrete mix specimens, the cylindrical shape of the size diameter $x$ length is 150 mm × 300 mm. For the splitting tensile test of the concrete, a loading rate of 4.5 kN/sec was applied in the transverse direction of the cylindrical specimens [70]. As a result, the splitting tensile is greater than the direct tensile but less than the flexural strength of the same concrete mix design.

Flexural strength, also known as concrete rupture, is used to determine the bending capability of concrete specimens. If the maximum aggregate size is less than 20 mm, a beam of the standard size of 100 mm × 100 mm $x$ 500 mm is used to analyze the flexural strength of the cast specimens. A two-point load was applied along the specimens' transverse direction for the test on the flexural testing machine [71].

The elastic modulus and the Poisson's ratio of the concrete mix are analyzed by testing on the cylindrical specimens. First, the uniaxial static load was applied vertically to the cylindrical specimens and found the cylinder's vertical and horizontal displacement and strength. Then, the

Poisson's ratio was calculated through the horizontal strain ratio of the vertical strain from the displacements. The elastic modulus is found through the load applied to the cylindrical specimens at about one-third of their strength and release, and going continuously through the same procedure often draws the stress-strain graph and finds the elastic modulus through the chord modulus as per the American standard code. Figure 4 shows the mechanical properties test pics of 4(a) compressive strength, 4(b) splitting tensile, 4(c) flexural strength, and 4(d) Poisson's ratio and elastic modulus.

*2.7. Nondestructive Tests.* The nondestructive test is also used to identify the specimen's strength without any destruction, and it primarily uses the rebound hammer test and the UPV test. The rebound hammer test based on the specimen's surface penetration is reflected by the specimen's surface hardness [72]. The UPV test propagates the ultrasonic pulse in the sample and measures the time travel duration to pass the specimen. The transducers are connected on two opposite sides of the specimen, where one works as an emitter and the other works as a receiver of ultrasonic pulse waves as per the Indian standard [73]. Figure 5 shows the nondestructive test pics of (a) rebound strength and (b) UPVT.

## 3. Results and Discussion

All the cast specimens of both concrete mixes were tested in the machines compared to the concrete mix's mechanical properties. In addition, the specimens of cubical, cylindrical, and beams were tested as per the Indian standards. The experimental work on GPC and OPC concrete mixes was conducted in the concrete laboratory of the Civil Engineering Department, Delhi Technological University, Delhi. It includes the slump value, compaction factor, setting time, density, drying shrinkage, compressive strength, splitting tensile, flexural strength, Poisson's ratio, elastic modulus, rebound strength, and UPV.

*3.1. Physical Properties.* The slump and compaction factor tests are used to analyze the workability of the fresh concrete mix. In both types of concrete, the slump values of both OPC and GPC concrete are the same at 75–100 mm, and the compaction factor of the OPC concrete is .89, whereas the GPC is .87 after mixing in the pan mixture for 3–5 minutes. The concrete mix's workability is increased by adding a superplasticizer to the mix without reducing the concrete's strength. The SNF-based superplasticizer does not harm the GPC specimen's strength [74]. It also increases microstructure development [75], but it is not beneficial at elevated temperatures [85–89]. The workability of the GPC decreases with the increment of the fineness of the fly ash [76], whereas it increases with the increment of the ratio of alkaline solution to fly ash [77]. The workability decreases with an increment in the alkaline ratio or molarity of the sodium hydroxide [78]. The setting time of the GPC is higher than that of conventional concrete. Figure 6(a) shows both the initial and final setting times. The setting time of the GPC decreases with the increment in the molarity of sodium hydroxide and GGBFS content in the mix design [79, 80].

*3.2. Chemical Properties.* The concrete sample cube's weight is used to calculate density before the compressive strength test after 28 days of casting. The density of the OPC concrete mix design increases with time, whereas the density of the GPC decreases at the same time. The maximum density of GPC is 2492 kg/m$^3$ found three days after the casting, whereas the maximum density of OPC concrete is 2462 kg/m$^3$ found 28 days after the casting. The concrete density with age is the inverse case in both concretes because GPC density decreases with increasing time while OPC density increases. Figure 6(c) shows the graph between the density and time in which the GPC sample density decreases with increasing time, but the OPC concrete density increases after up to 28 days of testing. The density of the concrete is increased by the addition of finer content in the mix-like nanoparticle materials. The drying shrinkage of conventional concrete is higher than that of GPC. Figure 6(b) shows the graph of the drying shrinkage of both concrete specimens. The conventional concrete specimens' drying shrinkage is initially lower than GPC, but it increases and lowers the GPC specimens' drying shrinkage.

*3.3. Compressive Strength.* The compressive strength of GPC and OPC concretes is similar in trends at 28 days' strength, but the GPC strength is much higher in the first three days' strength than the OPC concrete, but the compressive strength of the concrete mix is similar around 28 days. The three-day compressive strength of GPC and OPC concrete is 23.2 MPa and 14.4 MPa, respectively, while the 28-day compressive strength of GPC and OPC concrete is 35 MPa and 35.6 MPa. Figure 6(d) depicts the compressive time graph for both concretes. The graph shows that the initial strength of the GPC is higher than the OPC concrete samples but shows similar strength at 28 days of compressive strength. The compressive strength of OPC concrete is increased by reducing water content, the addition of superplasticizer, an increment in cement content, and silica fumes in the mix design. The compressive strength of the GPC depends on various parameters such as the molarity of NaOH, alkaline ratio, curing condition, curing temperature, curing time, water content, and superplasticizer. The compressive strength of the GPC increases with the increment of NaOH concentration in the mix design [81, 82]. It increases with the increment of the GGBFS content, curing temperature, curing period, mixing period, and fineness of fly ash [18, 83].

*3.4. Splitting Tensile.* The splitting tensile strength of the concrete mix designs was found by testing the mix design's cylindrical specimens in the compression testing machine at a loading rate of 4.5 kN/sec statically. The splitting tensile strength of the GPC is higher compared to the OPC concrete mix specimens. At 3, 7, 14, and 28 days, the splitting tensile of the OPC concrete is 1.5 MPa, 3 MPa, 3.5 MPa, and

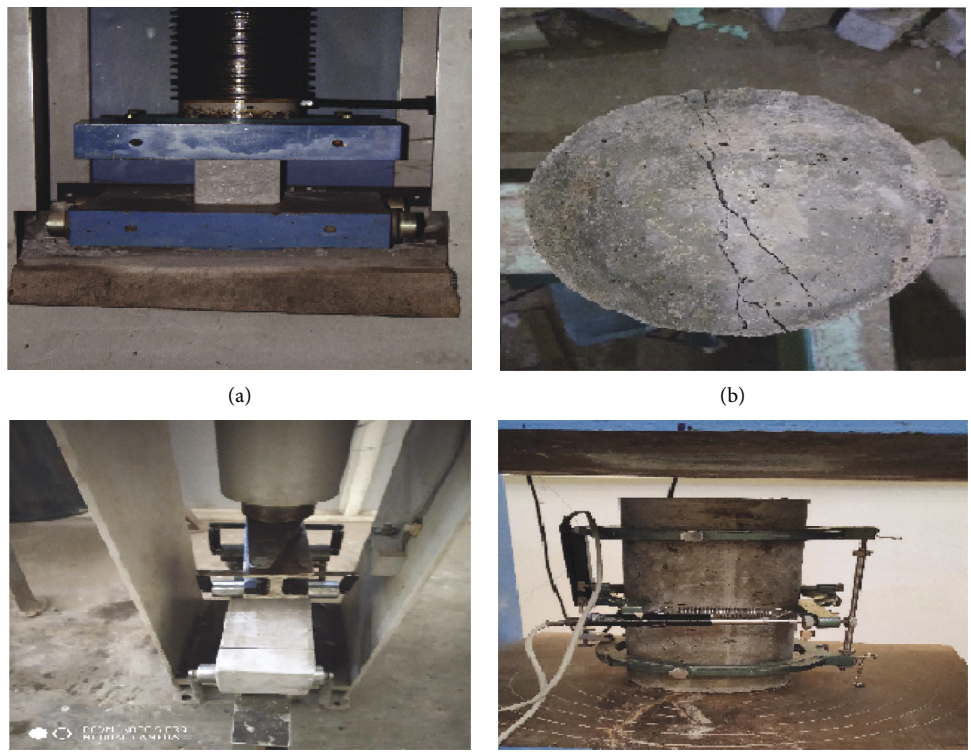

(a) (b) (c) (d)

Figure 4: Mechanical properties test pictures of (a) compressive strength; (b) splitting tensile; (c) flexural strength; and (d) Poisson's ratio and elastic modulus.

(a) (b)

Figure 5: Nondestructive tests pics of (a) rebound strength and (b) UPVT.

3.8 MPa, respectively, whereas the splitting tensile of the GPC is 2.6 MPa, 3.2 MPa, 3.9 MPa, and 4.2 MPa, respectively. Thus, the splitting strength of the GPC is slightly higher than that of the OPC concrete for the same compressive strength mix. Figure 6(e) depicts the time-dependent splitting tensile of both concretes. It shows that the GPC samples have higher splitting tensile compared to the OPC concrete samples. The GPC specimens show an initial high strength after 7 days, but after 28 days, they show similar trends. As the sand/fly ash ratio is increased, the tensile strength gradually decreases [84]. The comparison of ACI standard code design strength and experimental test results of geopolymer concrete tensile strength revealed that the splitting tensile strength of GPC matched the design

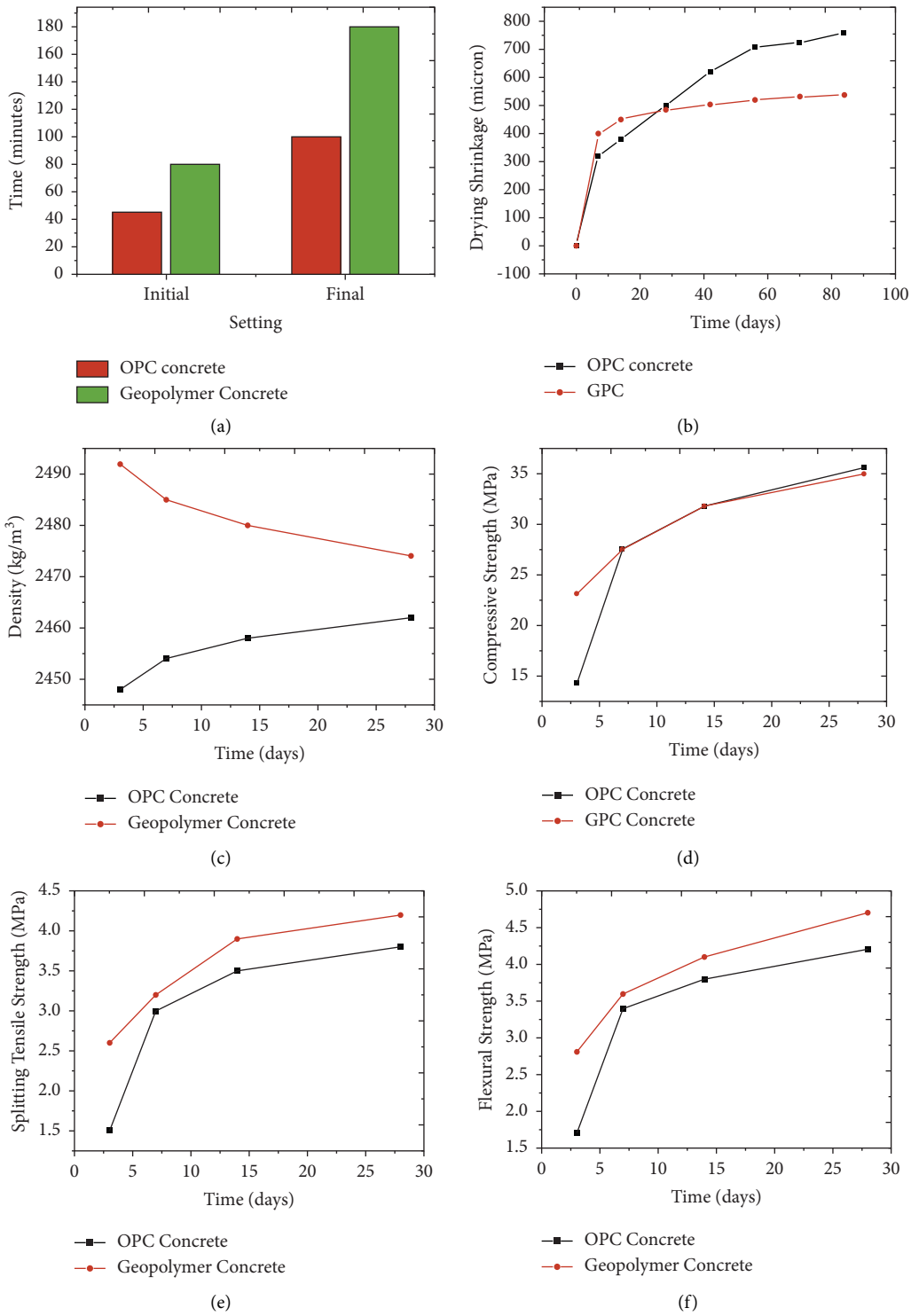


Figure 6: (a) Setting time of concretes; (b) drying shrinkage of the concretes; (c) density variations with time; (d) compressive strength of GPC and OPC concrete; (e) splitting tensile of the GPC and OPC concrete; and (f) flexural strength of GPC and OPC concrete.

specifications specified by the ACI standard [85]. In terms of tensile strength, the geopolymer concrete outperformed the OPC concrete [86, 87].

*3.5. Flexural Strength.* The flexural strength of the concrete mix designs is identified by testing the beam samples of the mix design in the flexural testing machine under a two-point load applied on the section of the beam in the transverse direction of the specimens. The flexural strength of the GPC specimens is slightly higher than the OPC concrete mix specimens. The flexural strength of OPC concrete is 1.7 MPa, 3.4 MPa, 3.8 MPa, and 4.2 MPa after 3, 7, 14, and 28 days, respectively, whereas the GPC flexural strength is 2.8 MPa,

3.6 MPa, 4.1 MPa, and 4.7 MPa after 3, 7, 14, and 28 days. Figure 6(f) describes the flexural strength and the time of both concretes. It shows that the GPC has higher flexural strength than OPC concrete samples in all tests. With normal curing, the inclusion of 5–6% nano-silica enhanced the tensile strength of GPC [88]. The GPC experimental findings using GGBFS and fly ash revealed that using GGBFS in the GPC matrix had a good effect on the direct tensile strength of GPC [89]. According to the literature research, the tensile strength of GPC concrete is superior to that of OPC concrete with the same compressive strength [90].

*3.6. Elastic Modulus and Poisson's Ratio.* The elastic modulus and the Poisson's ratio of the concrete mix design are identified by testing the cylindrical specimens of the mix in the compression testing machine with vertical and horizontal extension meters. The load was applied along the vertical direction of the specimens statically in the machine. To calculate the lateral and linear deformation of specimens subjected to strain after failure, the lateral strain ratio to the linear strain shows the Poisson's ratio of the concrete mix design, whereas the load applied one-third of the failure load to the specimens, reduced the load, and continued the same procedure many times. The slope of the initial stress-strain curve describes the elastic modulus of the concrete mix design. The GPC and OPC concrete mix designs' elastic modulus was tested 28 days after casting the specimen moulds. The OPC concrete's elastic modulus is slightly higher than the GPC mix design, whereas the Poisson's ratio of the OPC concrete is slightly lower than the GPC mix design. The elastic modulus of the OPC concrete and GPC is 26.3 GPa and 23.4 GPa, respectively, whereas the Poisson's ratio of the OPC concrete and GPC is .15 and .17, respectively. Figure 4(d) shows the setup to determine the Poisson's ratio and elastic modulus of the concrete mix cylindrical samples.

*3.7. Nondestructive Tests*

*3.7.1. Rebound Strength.* The rebound strength test is generally used in the field as a nondestructive test. It is based on the hammer striking on the specimen's surface with some IS code provisions and shows the rebound value. The rebound hammer is struck on the specimen surface ten times continuously, and the rebound gives the average rebound value and the rebound strength of the specimens according to Indian standards. The rebound strength shows similar trends to the mix's compressive strength, but the rebound strength shows a little higher value. For example, the initial three-day strength of GPC is higher than the OPC concrete mix but shows somewhat lower strength than the OPC concrete. Figure 7(a) describes the graph of the rebound strength of both GPC and OPC concrete.

*3.7.2. UPV Test.* The UPV test is vital in the nondestructive test method because it provides strength and crack information for the existing structures. The UPV test needs only two opposite sides of specimens to propagate ultrasonic pulse waves in a clean condition. Because rebound tests are based on surface hardness, they are only used on specimens with a thickness of up to 300 mm. The UPV test is primarily used in consulting work on existing concrete structures. The UPV of the specimens increases with hardness, which is directly proportional to their strength. Figure 7(b) describes the graph of the UPV test results of both GPC and OPC concrete mix samples. It shows similar trends in GPC and OPC concrete to the rebound strength graph.

*3.8. TGA (Thermo Gravimetric Analysis).* The TGA test does the thermal analysis of materials by increasing the temperature by 10°C per second up to 900°C and checking the derivative of weight reduction with the temperature. The apparatus shows notes of the weight reduction of the material with increasing temperature in a graphical form. The two parameters are represented in a single graph with different $y$-axes but a single $x$-axis, where one $y$-axis represents the derivative weight percentage and the other represents the weight percentage reduction with temperature. The GPC matrix is highly stable at elevated temperatures without failure compared to the OPC concrete matrix. Figure 8 describes the graph of TGA-DTG of GPC concrete up to the temperature of 850°C. It shows that the weight decreases with increasing temperature, but the GPC matrix is highly stable up to 850°C, and it shows the retained material is 92% of the original at 850°C. The DTG graph shows that the weight reduction with temperature is nonlinear, varying from negative to positive.

## 4. Mechanical Properties Correlation

The correlation is created by analyzing data on mechanical properties obtained from destructive laboratory tests. The linear regression analysis of compressive strength, splitting tensile, and flexural tensile strength showed the correlation equation and compared it to the Indian standard correlation equations.

*4.1. Correlation between the Compressive Strength and Splitting Tensile.* The correlation between splitting tensile and compressive strength is proposed in equation (1). It is produced as a result of regression analysis of data generated by destructive testing in the laboratory. In the state-of-the-art of high-strength concrete [91], the ACI committee gives equation (2), and a committee of the European Code International gives equation (3) in the model code of 1990 [92]. Equation (4) was introduced by an ACI standard and report for building code requirements for structural concrete [93]. The graph of the correlation between compressive strength and splitting tensile strength is shown in Figure 9. A regression analysis of the test data yields the correlation equation.

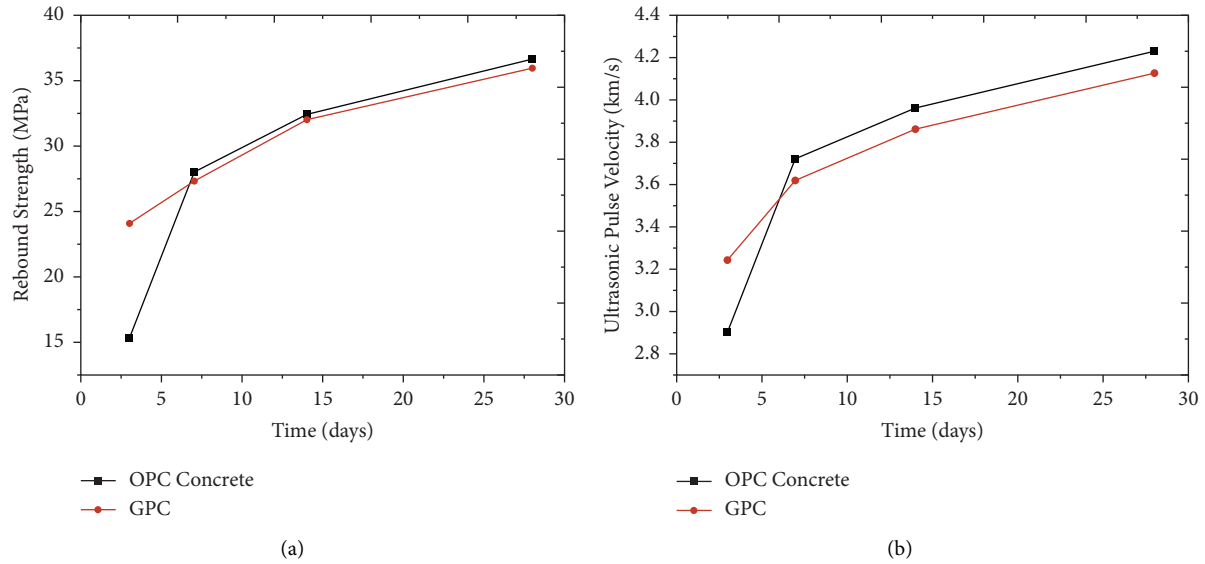


Figure 7: (a) Graph of OPC concrete and GPC rebound strength; and (b) graph of OPC concrete and GPC UPV test.

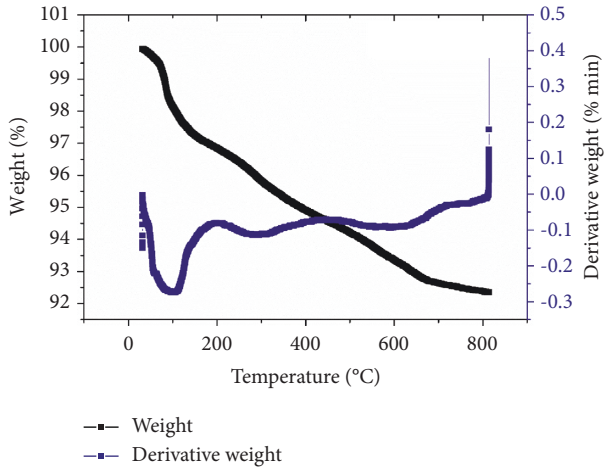


Figure 8: Graph of TGA-DTG test of GPC mix.

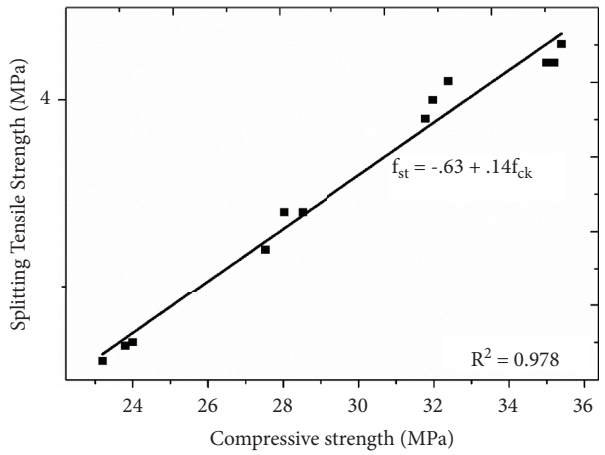


Figure 9: Graph of correlation between compressive strength and splitting tensile.

$$\text{Propose d: } f_{st} = -63 + 14 f_{ck}, \tag{1}$$

$$ACI363R - 92: f_{st} = 0.59\sqrt{f_c}, \tag{2}$$

$$CEB - FIP: f_{st} = 0.301 f_c^{0.67}, \tag{3}$$

$$ACI318 - 14: f_{st} = 0.56 f_c^{0.5}. \tag{4}$$

*4.2. Correlation between Compressive Strength and Flexural Strength.* The correlation between the compressive strength and flexural description by equation (5) is through the regression analysis of the test data. In the publication of the state-of-the-art of high strength concrete, the ACI committee included equation (6). A standard report presented on the code for the design of concrete in a structure introduces the equation (7) of correlation. The Australian code for reinforced concrete design presented equation (8), and the Indian code introduced equation (9) between flexural strength and compressive strength [94, 95]. The flexural strength is always about 10%–20% of the compressive strength. The tested data also lie between these values. The graph of the correlation equation between flexural strength and compressive strength proposed by the tested data is shown in Figure 10.

$$\text{Propose d: } f_{fs} = -1.03 + 16 f_{cs}, \tag{5}$$

$$ACI363R - 92: f_{fs} = 0.94\sqrt{f_c}, \tag{6}$$

$$ACI318 - 99: f_{fs} = 0.62\sqrt{f_c}, \tag{7}$$

$$AS3600: f_{fs} = 0.6\sqrt{f_c}, \tag{8}$$

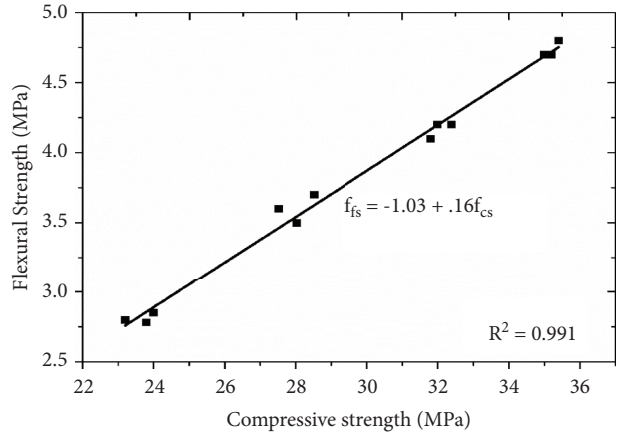


Figure 10: Graph of correlation between compressive strength and flexural strength.

Table 3: Embodied energy calculation of GPC and OPC.

| Constituents | Embodied energy (MJ/kg) | OPC concrete | | Geopolymer concrete | |
|---|---|---|---|---|---|
| | | Mix content (kg/m$^3$) | Embodied energy content (MJ/kg) | Mix content (kg/m$^3$) | Embodied energy content (MJ/kg) |
| OPC | 4.6 | 370 | 1702 | — | — |
| Fly ash | 0.0 | — | — | 303.75 | 00 |
| GGBFS | 0.2 | — | — | 101.25 | 31.38 |
| NaOH | 20.5 | — | — | 40.5 | 830.25 |
| $Na_2SiO_3$ | 5.37 | — | — | 101.25 | 543.71 |
| Fine aggregate | 0.02 | 683 | 13.66 | 683 | 13.66 |
| Coarse aggregate | 0.22 | 1289 | 283.58 | 1269 | 279.18 |
| Water | 0.0 | 148 | 00 | 40.5 | 00 |
| Superplasticiser | 12.6 | 3.7 | 46.62 | 4.05 | 51.03 |
| | Total | 2493.7 | 2045.86 MJ/m$^3$ | 2543.7 | 1749.21 MJ/m$^3$ |

$$IS456 - 2000: \ f_{fs} = 0.7\sqrt{f_c}. \tag{9}$$

## 5. Sustainability Analysis

Sustainable development is essential in the present scenario. This vast volume of industrial solid waste is now created, necessitating this trash in development activities. The use of industrial solid waste decreases carbon footprints and, as a result, indirectly lowers the use of high embodied energy items. For example, the embodied energy in the dry process of OPC cement is approximately 4.6 MJ/kg, whereas fly ash and slag have no embodied energy. By replacing the OPC, industrial solid waste fly ash and slag are used as the binder in concrete, and those wastes are activated by a chemical solution of sodium hydroxide and sodium silicate. As a result, the GPC has less embodied energy than the OPC concrete [96–98]. Table 3 shows the embodied energy calculation for both concrete and concrete. The embodied energy of all constituents of concrete is calculated based on the reference papers.

## 6. Cost Analysis

The concrete cost was calculated by the number of the constituents present in the concrete mix design, and then, after calculating the rate of all individual constituent prices, the concrete mix design cost was found. The cost of the GPC at a bulk level reduced the cost of up to 40% of the OPC concrete. The cost of the OPC of 1 m$^3$ is Rs. 3758, whereas the cost of the GPC of 1 m$^3$ is Rs. 2230. The cost estimate only includes the materials and excludes the human resources. Table 4 describes all the calculations of the cost of the materials and concrete. Materials and concrete costs are critical in the construction industry because construction projects are always more expensive. The project's economy always matters and goes to the optimum point, which is essential for the project's lower cost. When compared to OPC concrete, GPC concrete is less expensive and emits less carbon dioxide. This is a new trend in the construction industry due to sustainable development properties. Thaarrini and Dhivya compared the cost of GPC to cement concrete.

OPC concrete is 11% more expensive than GPC for better quality concrete. GPC costs 1.7% more than cement concrete for grades up to 30 MPa [99]. Through his

Table 4: Cost analysis of the GPC and OPC concrete.

| Constituents | Cost rate (Rs./kg) | OPC concrete | | Geopolymer concrete | |
|---|---|---|---|---|---|
| | | Mix content ($kg/m^3$) | Cost of the constituent ($Rs./m^3$) | Mix content ($kg/m^3$) | Cost of the constituent ($Rs./m^3$) |
| OPC | 7.6 | 370 | 2812 | — | — |
| Fly ash | 0.7 | — | — | 303.75 | 212.62 |
| GGBFS | 2.5 | — | — | 101.25 | 253.13 |
| NaOH | 10.05 | — | — | 40.5 | 407.03 |
| $Na_2SiO_3$ | 10 | — | — | 101.25 | 1012.5 |
| Fine aggregate | 0.25 | 683 | 170.75 | 683 | 170.75 |
| Coarse aggregate | 0.525 | 1289 | 676.72 | 1269 | 666.23 |
| Water | 0.0 | 148 | 00 | 40.5 | 00 |
| Superplasticiser | 26.67 | 3.7 | 98.68 | 4.05 | 108.01 |
| | Total | 2493.7 | Rs. $3758.15/m^3$ | 2543.7 | Rs. $2230.27/m^3$ |


Figure 11: Picture of short description of the GPC conclusion.

experimental analysis, McLellan et al. discovered that using fly ash-based GPC decreases building costs and greenhouse gas emissions by 7% and 64%, respectively. The cost of producing GGBS GPC was discovered to be 7% more than the cost of producing OPC-based concrete [100, 101]. Assi et al. developed a novel mix design approach for fly ash-based GPC that reduced construction costs by 50% [102].

## 7. Conclusions

After the experimental, sustainability, and cost investigations, they concluded the following:

(i) In both types of concrete, the slump value of both OPC concrete and GPC is the same, 75–100 mm, and the compaction factor of the OPC concrete is .89, whereas the GPC is .87 after mixing in the pan mixture for 3–5 minutes. The setting time of the GPC specimens is higher than the OPC concrete specimens.

(ii) The density of the OPC concrete mix design increases with time, whereas the density of the GPC decreases at the same time, and the drying shrinkage of the OPC concrete specimens is higher than the GPC specimens, but initially, its lower value before the 28-days test.

(iii) The compressive strength of the GPC and OPC concretes is similar in trends at the 28-day strength but not at the initial three-day strength; the GPC strength is much higher than the OPC concrete, but the compressive strength of the concrete mix becomes more similar around 28 days.

(iv) The splitting tensile and flexural strength of the GPC is slightly higher than the OPC concrete mix specimens. Similarly, the OPC concrete's elastic modulus is slightly higher than the GPC mix design, whereas the Poisson's ratio of the OPC concrete is slightly lower than the GPC mix design.

(v) The rebound strength shows similar trends to the mix's compressive strength, but the rebound strength shows a little higher value. The UPV results show similar trends in GPC and OPC concrete to the rebound strength graph.

(vi) The TGA test shows that the weight decreases with increasing temperature, but the GPC matrix is highly stable up to 850°C, and it shows the retained material is 92% of the original at 850°C.

(vii) The GPC has less embodied energy compared to the OPC concrete.

(viii) The cost of the GPC at a bulk level reduced the cost of up to 40% of the OPC concrete. The cost of the OPC concrete of 1 $m^3$ is Rs. 3758, whereas the cost of the GPC of 1 $m^3$ is Rs. 2230.

(ix) The experimental results proposed that the correlation equation between compressive strength and splitting tensile was $f_{st} = -.63 + .14f_{ck,}$ and the correlation equation between compressive strength and flexural strength was $f_{fs} = -1.03 + .16f_{cs.}$

(x) After the research, the conclusion is represented in the graph form in Figure 11.

## Data Availability

All data are included in the article.

## Additional Points

The authors also focus on a brief investigation of geopolymer concrete in an application. The microstructural characterization of these hybrid reinforced composites with low calcium geopolymer concrete is performed.

## Conflicts of Interest

The authors declare that there are no conflicts of interest.

## Acknowledgments

The experimental testing was supported by the Civil Engineering Department, Delhi Technological University, New Delhi, India.

## References

[1] Central Electricity Authority, *Flyash Generation at Coal/ lignite Based thermal Power Stations and its Utilization in the Country*, 2019.

[2] I. Ismail, S. A. Bernal, J. L. Provis, S. Hamdan, and J. S. J. van Deventer, "Microstructural changes in alkali-activated fly ash/slag geopolymers with sulfate exposure," *Materials and Structures*, vol. 46, no. 3, pp. 361–373, 2013.

[3] C. Chotetanorm, P. Chindaprasirt, V. Sata, S. Rukzon, and A. Sathonsaowaphak, "High-calcium bottom ash geopolymer: sorptivity, pore size, and resistance to sodium sulfate attack," *Journal of Materials in Civil Engineering*, vol. 25, no. 1, pp. 105–111, 2013.

[4] W. G. Valencia Saavedra, D. E. Angulo, and R. Mejía de Gutiérrez, "Fly ash slag geopolymer concrete: resistance to sodium and magnesium sulfate attack," *Journal of Materials in Civil Engineering*, vol. 28, no. 12, pp. 1–9, 2016.

[5] M. A. R. Bhutta, W. M. Hussin, M. Azreen, and M. M. Tahir, "Sulphate resistance of geopolymer concrete prepared from blended waste fuel ash," *Journal of Materials in Civil Engineering*, vol. 26, no. 11, pp. 1–6, 2014.

[6] P. Duxson, J. L. Provis, G. C. Lukey, S. W. Mallicoat, W. M. Kriven, and J. S. van Deventer, "Understanding the relationship between geopolymer composition, microstructure and mechanical properties," *Colloids and Surfaces A: Physicochemical and Engineering Aspects*, vol. 269, no. 1-3, pp. 47–58, 2005.

[7] G. Nagalia, Y. Park, A. Abolmaali, and P. Aswath, "Compressive strength and microstructural properties of fly ash – based geopolymer concrete," *Journal of Materials in Civil Engineering*, vol. 28, no. 12, pp. 1–11, 2016.

[8] G. S. Ryu, Y. B. Lee, K. T. Koh, and Y. S. Chung, "The mechanical properties of fly ash-based geopolymer concrete with alkaline activators," *Construction and Building Materials*, vol. 47, pp. 409–418, 2013.

[9] J. G. Jang, N. K. Lee, and H. K. Lee, "Fresh and hardened properties of alkali-activated fly ash/slag pastes with superplasticizers," *Construction and Building Materials*, vol. 50, pp. 169–176, 2014.

[10] P. Topark-Ngarm, P. Chindaprasirt, and V. Sata, "Setting time, strength, and bond of high-calcium fly ash geopolymer concrete," *Journal of Materials in Civil Engineering*, vol. 27, pp. 1–7, 2015.

[11] D. Hardjito, S. E. Wallah, D. M. J. Sumajouw, and B. V. Rangan, "On the development of fly ash-based geopolymer concrete," *ACI Materials Journal*, vol. 101, pp. 467–472, 2004.

[12] S. V. Patankar, Y. M. Ghugal, and S. S. Jamkar, "Effect of concentration of sodium hydroxide and degree of heat curing on fly ash-based geopolymer mortar," *Indian Journal of Materials Science*, vol. 2014, pp. 1–6, 2014.

[13] P. Nath and P. K. Sarker, "Effect of GGBFS on setting, workability and early strength properties of fly ash geopolymer concrete cured in ambient condition," *Construction and Building Materials*, vol. 66, pp. 163–171, 2014.

[14] P. Rovnaník, "Effect of curing temperature on the development of hard structure of metakaolin-based geopolymer," *Construction and Building Materials*, vol. 24, no. 7, pp. 1176–1183, 2010.

[15] P. Nath and P. K. Sarker, "Flexural strength and elastic modulus of ambient-cured blended low-calcium fly ash geopolymer concrete," *Construction and Building Materials*, vol. 130, pp. 22–31, 2017.

[16] S. Kumar, R. Kumar, and S. P. Mehrotra, "Influence of granulated blast furnace slag on the reaction, structure and properties of flyash-based geopolymer," *Journal of Materials Science*, vol. 45, no. 3, pp. 607–615, 2010.

[17] A. Sathonsaowaphak, P. Chindaprasirt, and K. Pimraksa, "Workability and strength of lignite bottom ash geopolymer mortar," *Journal of Hazardous Materials*, vol. 168, no. 1, pp. 44–50, 2009.

[18] S. S. Jamkar and Y. M. Ghugal Svp, "Effect of fineness of fly ash on flow and compressive strength of geopolymer concrete," *Indian Concrete journal*, vol. 87, no. 4, pp. 57–62, 2013.

[19] S. Luhar and U. Khandelwal, "A study on water absorption and sorptivity of geopolymer concrete," *International Journal of Civil Engineering*, vol. 2, no. 8, pp. 1–9, 2015.

[20] N. A. Lloyd and B. V. Rangan, "Geopolymer concrete with fly ash," in *Proceedings of the Second International Conference on Sustainable Construction Materials and Technologies*, pp. 1–7, 2010.

[21] D. S. Perera, E. R. Vance, O. Uchida, and K. S. Finnie, "Influence of curing schedule on the integrity of geopolymers," *Journal of Materials Science*, vol. 42, no. 9, pp. 3099–3106, 2007.

[22] D. Bondar, C. J. Lynsdale, N. B. Milestone, and N. Hassani, "Sulfate resistance of alkali activated pozzolans," *International Journal of Concrete Structures and Materials*, vol. 9, no. 2, pp. 145–158, 2015.

[23] D. Bondar, C. J. Lynsdale, N. B. Milestone, and N. Hassani, "Engineering properties of alkali activated natural pozzolan concrete," *Second Int Conf Sustain Constr Mater Technol*, vol. 108, pp. 1–10, 2010.

[24] N. K. Lee, J. G. Jang, and H. K. Lee, "Shrinkage characteristics of alkali-activated fly ash/slag paste and mortar at early ages," *Cement and Concrete Composites*, vol. 53, pp. 239–248, 2014.

[25] K. U. Ambikakumari Sanalkumar, M. Lahoti, and E. H. Yang, "Investigating the potential reactivity of fly ash for geopolymerization," *Construction and Building Materials*, vol. 225, pp. 283–291, 2019.

[26] Y. C. Ding, T. W. Cheng, and Y. S. Dai, "Application of geopolymer paste for concrete repair," *Structural Concrete*, vol. 18, no. 4, pp. 561–570, 2017.

[27] Z. Pan, J. G. Sanjayan, and F. Collins, "Effect of transient creep on compressive strength of geopolymer concrete for elevated temperature exposure," *Cement and Concrete Research*, vol. 56, pp. 182–189, 2014.

[28] K. Upreti, M. Verma, M. Agrawal et al., "Prediction of mechanical strength by using an artificial neural network and random forest algorithm," *Journal of Nanomaterials*, vol. 2022, pp. 1–12, 2022.

[29] A. Chouksey, M. Verma, N. Dev, I. Rahman, and K. Upreti, "An investigation on the effect of curing conditions on the mechanical and microstructural properties of the geopolymer concrete," *Materials Research Express*, vol. 9, no. 5, Article ID 55003, 2022.

[30] R. Kumar, M. Verma, and N. Dev, "Investigation of fresh, mechanical, and impact resistance properties of rubberized concrete," in *Proceedings of the International E-Conference on Sustainable Development & Recent Trends in Civil Engineering*, pp. 88–94, delhi, India, January 2022.

[31] M. Verma and M. Nigam, "Mechanical behaviour of self compacting and self curing concrete," *International Journal Innovation Research Science Engineer Technology*, vol. 6, pp. 14361–14366, 2017.

[32] M. Verma, "Experimental investigation on the properties of Geopolymer concrete after replacement of river sand with the M-sand," in *Proceedings of the International E-Conference on Sustainable Development & Recent Trends in Civil Engineering*, pp. 46–54, delhi, India, January 2022.

[33] R. Kumar, M. Verma, and N. Dev, "Investigation on the effect of seawater condition, sulphate attack, acid attack, freezet-haw condition, and wetting–drying on the geopolymer concrete," *Iranian Journal of Science and Technology, Transactions of Civil Engineering*, vol. 46, no. 4, pp. 2823–2853, 2021.

[34] M. Verma and N. Dev, "Effect of liquid to binder ratio and curing temperature on the engineering properties of the geopolymer concrete," *Silicon*, vol. 14, no. 4, pp. 1743–1757, 2022.

[35] A. Chouksey, M. Verma, N. Dev, I. Rahman, and K. Upreti, "An investigation on the effect of curing conditions on the mechanical and microstructural properties of the geopolymer concrete," *Materials Research Express*, vol. 9, no. 5, Article ID 55003, 2022.

[36] M. Verma and N. Dev, "Geopolymer concrete: a way of sustainable construction," *International Journal of Innovative Research in Advanced Engineering*, vol. 5, pp. 201–205, 2018.

[37] M. Verma and N. Dev, "Effect of SNF-based superplasticizer on physical, mechanical and thermal properties of the geopolymer concrete," *Silicon*, vol. 14, no. 3, pp. 965–975, 2021.

[38] M. Verma and N. Dev, "Geopolymer Concrete: A Sustainable and Economic Concrete via Experimental Analysis," *Research square*, pp. 1–39, 2021.

[39] N. Juneja and K. Upreti, "An Introduction to Few Soft Computing Techniques to Predict Software Quality," in *Proceedings of the 2017 2nd Int Conf Telecommun Networks*, Noida, India, August 2017.

[40] J. Ananthi, N. Sengottaiyan, S. Anbukaruppusamy, K. Upreti, and A. K. Dubey, "Forest fire prediction using IoT and deep learning," *International Journal of Advanced Technology and Engineering Exploration*, vol. 9, pp. 246–256, 2022.

[41] K. Upreti, U. K. Singh, R. Jain, K. Kaur, and A. K. Sharma, "Fuzzy logic based support vector regression (SVR) model for software cost estimation using machine learning," *ICT Systems and Sustainability*, vol. 321, pp. 917–927, 2022.

[42] M. Verma and N. Dev, "Sodium hydroxide effect on the mechanical properties of flyash-slag based geopolymer concrete," *Structural Concrete*, vol. 22, no. S1, pp. E368–E379, 2021.

[43] M. Verma, N. Dev, I. Rahman, M. Nigam, M. Ahmed, and J. Mallick, "Geopolymer concrete: a material for sustainable development in Indian construction industries," *Crystals*, vol. 12, no. 4, p. 514, 2022.

[44] M. Verma and N. Dev, "Review on the effect of different parameters on behavior of Geopolymer Concrete," *Int J Innov Res Sci Eng Technol*, vol. 6, pp. 11276–11281, 2017.

[45] M. Verma and N. Dev, "Effect of superplasticiser on physical, chemical and mechanical properties of the geopolymer concrete," *Challenges of Resilient and Sustainable Infrastructure Development in Emerging Economies*, pp. 1185–1191, Kolkata, India, 2020.

[46] M. Verma and N. Dev, "Effect of ground granulated blast furnace slag and fly ash ratio and the curing conditions on the mechanical properties of geopolymer concrete," *Structural Concrete*, vol. 23, no. 4, pp. 2015–2029, 2021.

[47] G. P. Hammond and C. I. Jones, "Embodied energy and carbon in construction materials," *Proceedings of the Institution of Civil Engineers - Energy*, vol. 161, no. 2, pp. 87–98, 2008.

[48] K. Kupwade-Patil and E. N. Allouche, "Examination of chloride-induced corrosion in reinforced geopolymer concretes," *Journal of Materials in Civil Engineering*, vol. 25, no. 10, pp. 1465–1476, 2013.

[49] K. Kupwade-Patil and E. N. Allouche, "Impact of alkali silica reaction on fly ash-based geopolymer concrete," *Journal of Materials in Civil Engineering*, vol. 25, no. 1, pp. 131–139, 2013.

[50] K. Arunkumar, M. Muthukannan, A. Suresh kumar, and A. Chithambar Ganesh, "Mitigation of waste rubber tire and waste wood ash by the production of rubberized low calcium waste wood ash based geopolymer concrete and influence of waste rubber fibre in setting properties and mechanical behavior," *Environmental Research*, vol. 194, Article ID 110661, 2021.

[51] R. Kumar, M. Verma, N. Dev, and N. Lamba, "Influence of chloride and sulfate solution on the long-term durability of modified rubberized concrete," *Journal of Applied Polymer Science*, pp. 1–15, 2022.

[52] M. Verma, A. Juneja, and D. Saini, "Effect of waste tyre rubber in the concrete," in *International E-Conference on Sustainable Development & Recent Trends in Civil Engineering*, pp. 99–103, 2022.

[53] *IS 8112 1989 (1990) 43 GRADE ORDINARY PORTLAND CEMENT - SPECIFICATION*, Bur Indian Stand, 1990.

[54] ASTM C 618 19, *Standard Specification for Coal Fly Ash and Raw or Calcined Natural Pozzolan for Use in concrete*, 2019.

[55] "IS 2386 (Part II) (1998) Methods of test for aggregates for concrete Part II Estimation of deleterious materials and organic impurties," *Bur Indian Stand*, vol. 2386, 1998.

[56] "IS 2386 (Part I) (1997) Methods of test for aggregates for concrete Part I Particle size and shape," *Bur Indian Stand*, vol. 2386, 1997.

[57] "IS 2386 (Part III) Methods of test for aggregates for concrete Part III Specific gravity, density, voids, absorption and bulking," *Bur Indian Stand*, vol. 2386, 1997.

[58] "IS 383 1970 Specification for coarse and fine aggregates from natural sources for concrete," *Bur Indian Stand*, pp. 1–20, 1997.
[59] "IS 2386 (Part IV) Methods of test for aggregates for concrete Part IV Mechanical Properties," *Bur Indian Stand*, vol. 2386, 1997.
[60] IS 2386 (PartV), *Methods of Test for Aggregates for concrete Part V Soundness*, Bur Indian Stand, 1997.
[61] *IS 9103 1999 CONCRETE ADMIXTURES-Specification*, Bur Indian Stand April, 1999.
[62] *IS 12119 1987 GENERAL REQUIREMENT FOR PAN MIXTURES FOR CONCRETE*, Bur Indian Stand, 1999.
[63] *IS 10262 2009 CONCRETE MIX PROPORTIONING - GUIDELINES*, Bur Indian Stand, 2009.
[64] "IS: 1199 - 1959 reaffirmed, IS 1199 1959," *METHODS OF SAMPLING AND ANALYSIS OF CONCRETE*, Bur Indian Stand, 1959.
[65] "IS 7325 1974 (1999) specification for apparatus for determining constituents of fresh concrete," *Bur Indian Stand*, pp. 1–12, 1999.
[66] *IS 7320 1974 Specification for concrete Slump Test Apparatus*, Bur Indian Stand, 2008, https://doi.org/10.1136/archdischild-2011-300172.
[67] "(unit weight), yield, and air content (gravimetric) of concrete," 2019, https://doi.org/10.1520/C0138 ASTM C138/C138M 17a (2019) Standard Test Method for Density ASTM Int 1–6.
[68] *IS 516 1959 METHODS OF TEST FOR STRENGTH OF CONCRETE*, Bur Indian Stand, 2004.
[69] "IS 10086 1982," *SPECIFICATION FOR MOULDS FOR USE IN TESTS OF CEMENT AND CONCRETE*, Bur Indian Stand, 2008.
[70] *IS 5816 1999 SPLITTING TENSILE STRENGTH OF CONCRETE - METHOD OF TEST*, Bur Indian Stand, 1999.
[71] "IS 9399 1979," *SPECIFICATION FOR APPARATUS FOR FLEXURAL TESTING OF CONCRETE*, Bur Indian Stand, 1979.
[72] *IS 13311-2 Method of Non-destructive Testing of concrete-methods of Test Part 2: Rebound Hammer*, Bur Indian Stand, 1992.
[73] IS 13311 (Part1), *Non-destructive Testing of concrete Methods of Test Part 1 Ultrasonic Pulse Velocity*, Bur Indian Stand, 1992.
[74] M. Albitar, P. Visintin, M. S. Mohamed Ali, and M. Drechsler, "Assessing behaviour of fresh and hardened geopolymer concrete mixed with class-F fly ash," *KSCE Journal of Civil Engineering*, vol. 19, no. 5, pp. 1445–1455, 2015.
[75] S. Demie, M. F. Nuruddin, and N. Shafiq, "Effects of microstructure characteristics of interfacial transition zone on the compressive strength of self-compacting geopolymer concrete," *Construction and Building Materials*, vol. 41, pp. 91–98, 2013.
[76] T. Phoo-ngernkham, C. Phiangphimai, N. Damrongwiriyanupap, S. Hanjitsuwan, J. Thumrongvut, and P. Chindaprasirt, "A mix design procedure for alkali-activated high-calcium fly ash concrete cured at ambient temperature," *Advances in Materials Science and Engineering*, vol. 2018, Article ID 2460403, 15 pages, 2018.
[77] C. A. Jeyasehar and M. Salahuddin, "Development of fly ash based geopolymer concrete precast elements," *Ministry of Environment and Forests of India and Annamalai University*, pp. 1–77, 2013.
[78] I. Perná, T. Hanzlicek, and M. Supova, "The identification of geopolymer affinity in specific cases of clay materials," *Applied Clay Science*, vol. 102, pp. 213–219, 2014.
[79] V. D. Cao, S. Pilehvar, C. Salas-bringas et al., "Micro-encapsulated phase change materials for enhancing the thermal performance of Portland cement concrete and geopolymer concrete for passive building applications," *Energy Conversion and Management*, vol. 133, pp. 56–66, 2017.
[80] B. S. Umniati, P. Risdanareni, F. Tarmizi, and Z. Zein, "Workability enhancement of geopolymer concrete through the use of retarder workability enhancement of geopolymer concrete through the use of retarder," in *Proceedings of the AIP Conference Proceedings*, pp. 1–9, Sepetember 2017.
[81] E. Najafi Kani and A. Allahverdi, "Effects of curing time and temperature on strength development of inorganic polymeric binder based on natural pozzolan," *Journal of Materials Science*, vol. 44, no. 12, pp. 3088–3097, 2009.
[82] C. Sreenivasulu, A. Ramakrishnaiah, and J. G. Jawahar, "M echanical P roperties of G eopolymer C oncrete," *International Journal of Advances in Engineering & Technology*, vol. 8, pp. 83–91, 2015.
[83] G. Nagalia, Y. Park, A. Abolmaali, and P. Aswath, "Compressive strength and microstructural properties of fly ash – based geopolymer concrete," *Journal of Materials in Civil Engineering*, vol. 28, no. 12, pp. 1–11, 2016.
[84] W. K. W. Lee and J. D. Deventer, "Chemical interactions between siliceous aggregates and low-Ca alkali-activated cements," *Cement and Concrete Research*, vol. 37, no. 6, pp. 844–855, 2007.
[85] X. Y. Zhuang, L. Chen, S. Komarneni et al., "Fly ash-based geopolymer: clean production, properties and applications," *Journal of Cleaner Production*, vol. 125, pp. 253–267, 2016.
[86] H. Y. Zhang, V. Kodur, B. Wu, L. Cao, and F. Wang, "Thermal behavior and mechanical properties of geopolymer mortar after exposure to elevated temperatures," *Construction and Building Materials*, vol. 109, pp. 17–24, 2016.
[87] Z. H. Zhang, H. J. Zhu, C. H. Zhou, and H. Wang, "Geopolymer from kaolin in China: an overview," *Applied Clay Science*, vol. 119, pp. 31–41, 2016.
[88] D. Adak, M. Sarkar, and S. Mandal, "Effect of nano-silica on strength and durability of fly ash based geopolymer mortar," *Construction and Building Materials*, vol. 70, pp. 453–459, 2014.
[89] A. Hassan, M. Arif, and M. Shariq, "Use of geopolymer concrete for a cleaner and sustainable environment – a review of mechanical properties and microstructure," *Journal of Cleaner Production*, vol. 223, pp. 704–728, 2019.
[90] F. Collins and J. G. Sanjayan, "Strength and shrinkage properties of alkali-activated slag concrete placed into a large column," *Cement and Concrete Research*, vol. 29, no. 5, pp. 659–666, 1999.
[91] H. G. Russell, A. R. Anderson, and J. O. Banning, *State-of-the-Art Report on High-Strength Concrete Reported by ACI Committee 363*, 1997.
[92] C. International, *ceb-fip-model-code-1990-design-code*, 1990.
[93] A. C. I. Committee, *Building Code Requirements for Structural Concrete*, pp. 318–414, 2014.
[94] C. Concrete, *Reinforced Concrete Design in Accordance with AS 3600—2009*, 2009.
[95] *IS 456 2000 PLAIN AND REINFORCED CONCRETE - CODE OF PRACTICE*, Bur Indian Stand, 2000.
[96] B. N. Varsha and S. J. K. R. Saranya, "Embodied energy of aggregates and masonry units produced around Bengaluru,

India," *International Journal of Advanced Science and Engineering Technology*, vol. 6, pp. 42–45, 2018.

[97] M. A. Gonzalez Stumpf, M. P. Kulakowski, L. G. Breitenbach, and F. Kirch, "A case study about embodied energy in concrete and structural masonry buildings," *Revista de la construcción*, vol. 13, no. 2, pp. 9–14, 2014.

[98] S. R. Anvekar, L. R. Manjunatha, S. R. Anvekar, S. Sagari, and K. Archana, "An economic and embodied energy comparison of geo-polymer, blended cement and traditional concretes," *J Civ Eng Technol Res*, vol. 1, pp. 33–40, 2014.

[99] T. Janardhanan, J. Thaarrini, S. Dhivya &, and S. Dhivya, "Comparative study on the production cost of geopolymer and conventional concretes," *International Journal of Civil Engineering Research*, vol. 7, pp. 117–124, 2016.

[100] B. C. McLellan, R. P. Williams, J. Lay, A. van Riessen, and G. D. Corder, "Costs and carbon emissions for geopolymer pastes in comparison to ordinary portland cement," *Journal of Cleaner Production*, vol. 19, no. 9-10, pp. 1080–1090, 2011.

[101] B. J. Mathew, M. Sudhakar, and C. Natarajan, "Strength , economic and sustainability characteristics of coal ash – GGBS based geopolymer concrete," *International Journal of Computational Engineering Research*, vol. 3, pp. 207–212, 2013.

[102] L. Assi, K. Carter, E. E. Deaver, R. Anay, and P. Ziehl, "Sustainable concrete: building a greener future," *Journal of Cleaner Production*, vol. 198, pp. 1641–1651, 2018.